Design and Joint Control of a Conjoined Biplane and Quadrotor

S.Schröter,* E.J.J.Smeur, and B.D.W. Remes

Delft University of Technology, 2629 HS, the Netherlands

ABSTRACT

Unmanned Aerial Vehicles (UAVs) have the potential to perform many different missions, some of which may require a large aircraft for endurance and a small aircraft for manoeuvrability in a building. This paper proposes a novel combination of a quadrotor and a hybrid biplane capable of joint hover, joint forward flight, and mid-air disassembly followed by separate flight. We investigate cooperative control strategies during joint flight that do not require any communication between the quadcopter and the biplane. This means that the two aircraft have their own independent control strategy based on their own sensors. Secondly, to avoid communication the biplane leads the flight and the goal for the quadrotor is to help in producing thrust and increasing stability. Three control strategies for the quadrotor are compared: a proportional angular rate damper, a proportional angular acceleration damper, and constant thrust without attitude control. Simulation and practical tests show that for intentional attitude changes of the biplane, the quadrotor rate- and angular acceleration damper strategies lead to a small performance degradation. However, the angular rate damper strategy for disturbance rejection has the lowest roll angle error and requires the smallest input command. The in-flight release is successfully tested in joint hover up to a forward pitch angle of -18 [deg].

1 INTRODUCTION

Unmanned Air Vehicles (UAVs) have increased in popularity and can serve various purposes, ranging from inspection of structures to traffic surveillance, and each type of UAV has its own distinguishing properties. Fixed-wing aircraft are known for their endurance and efficiency, but they require a constant horizontal speed to stay in the air. Multirotors are more agile and are capable of hover, but they lack endurance. A hybrid aircraft can hover and has wings for efficient forward flight, combining the best of both worlds. However, a hybrid aircraft with large wings is not well-equipped to maneuver inside a building. This poses a problem for missions where the goal is to fly inside a building after a long-distance transit flight.

One solution could be to drop a smaller UAV out of a bigger one. In-air deployment of a fixed-wing from a quadrotor has been shown by Boeing[1]. Voskuijl et al. investigated morphing UAVs being dropped as armaments out of (military) airplanes [1]. A downside of this approach is that the smaller UAV is carried around as dead weight, and does not contribute to the propulsion until it is deployed. This could lead to over-dimensioning of the carrier aircraft. Cooperative flight is somewhat similar to airborne docking [2], formation flight with communication [3], and without communication [4]. However, in these works the individual UAVs are typically not rigidly attached and can maneuver independently to some degree.

Examples of cooperative flight with modular joint airframes are the Modquad [5] and the Distributed Flight Array [6]. Both airframes are capable of assembling in-flight, and the latest version of the Modquad is even capable of in-flight disassembly [7]. However, all aircraft used in this research have the same size and function, without a focus on combining different types of UAVs to obtain better endurance and flexibility in operation.

In this paper, we propose a combination of a quadrotor and a hybrid aircraft with a fixed wing, that can fly together, both contributing to stabilization and propulsion, and can disassemble in-flight into a fully functional quadcopter and hybrid aircraft. Figure 1 graphically shows the various stages in which the joint structure would fly.

For a UAV's attitude and trajectory control specifically, many options exist. The most popular method is PID control [8], but also model-based controllers exist for UAVs [9]. For hybrid aircraft, Incremental Nonlinear Dynamic Inversion (INDI) has proven to be very effective [10]. Especially in the hover phase, hybrid aircraft are extremely susceptible to external disturbances [11, 12], and INDI has better disturbance rejection compared to PID [13].

Different forms of communication have been used in all forms of cooperative flight between different aircraft, but this has proven to have its challenges, such as time delays, false information and noise. Wired communication between the aircraft would be less of a liability, but a way to work around all these problems is to avoid any communication altogether. That is why a control strategy is proposed in this paper where

---

*Email address: shawn@schroter.info

[1] https://www.boeing.com/features/2016/09/catch-and-release-flares-09-16.page

both aircraft have no communication with each other. This way, the joint structure becomes more reliable, which is important for long-distance operations.

Two main questions will be dealt with: how can the joint vehicle be controlled and how can the two aircraft be disassembled in mid-air?
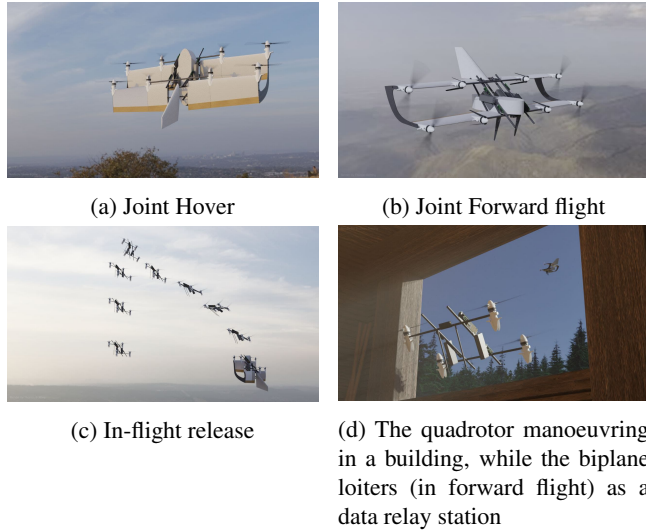
(a) Joint Hover

(b) Joint Forward flight

(c) In-flight release

(d) The quadrotor manoeuvring in a building, while the biplane loiters (in forward flight) as a data relay station

Figure 1: Different phases of the joint structure's activities

2 JOINT STRUCTURE DESIGN

This section will cover three main parts of the structure in more detail; The hybrid biplane, the quadrotor and the release mechanism.
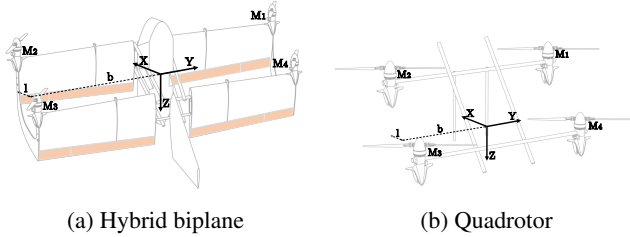

(a) Hybrid biplane

(b) Quadrotor

Figure 2: Schematic drawing of the hybrid biplane and quadrotor with axis definitions. The control surface are accentuated in light orange. M_i illustrates the ith rotor actuators.

2.1 Hybrid biplane

The biplane is a tailsitter hybrid aircraft. For this aircraft, the Nederdrone formed the basis of the biplane design [10]. The biplane has eight mounting points for rotors and four control surfaces. The four outer mounting points are fixed, and the four inner mounting points are part of the release mechanism. The control surfaces control the airflow around the wings, providing moments around the Y- and Z-axes. In

the hover phase, this airflow is created by the rotors. Table 1 presents an overview of the different parts of the hybrid biplane. The reference frame is defined in hover state, as shown in Figure 2a. Forward flight would mean a $-90[deg]$ pitch angle.

| Type of Hardware	Brand	Item
Motor	T-Motor	MN3510
Radio Control link	TBS	Crossfire nano
Telemetry link	Herelink	Herelink
Electronic Speed Controller	T-Motor	f45A 32_bit
Propeller	T-motor	MF1302
Flight controller	Holybro	Pixhawk4
Battery	Extron	2x 6s 4.5 Ah

Table 1: Different components of the biplane

2.2 Quadrotor

The design of the quadrotor is derived from the dimensions of the biplane. This means that on the four inner mounting points of the biplane the four rotors of the quadrotor are placed. Four hollow carbon rods connect the four rotors. The rods are placed in such a way that the quadrotor would be able to release without being obstructed by the biplane. Furthermore, two solid carbon guiding support a more consistent release and serve as landing legs. A schematic overview of the quadrotor is shown in Figure 2b. Figure 1c shows the release if the biplane is in hover. The powertrain is similar to the biplane. One difference is that the quadrotor uses two 3s 4500 mAh batteries, connected in series.

2.3 Release mechanism

The release mechanism is mounted just underneath the motors of the quadrotor. At each of the four motor locations, two copper pins fix the quadrotor to the biplane. The release system is a slider-crank mechanism powered by a servo. Since the quadrotor needs to drastically change its method of control once it detaches from the biplane, it is given control over the release mechanism.
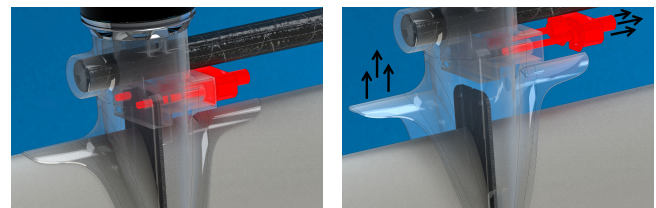
(a) Closed position - The pin is locked in the carbon plate.

(b) Lift-off of the quadrotor

Figure 3: Closed position and release of the RC servo Release Mechanism

Figure 3 graphically shows how the release system enables the quadrotor to separate from the biplane. Once the pins are out, the motor mount slides in the direction of the

thrust force. A thrust difference between the biplane and the quadrotor then leads to separation. The guiding tubes of the quadrotor help the thrust force of the quadrotor to stay approximately opposite to the weight force of the biplane.

3 MODEL STRUCTURE

This section will explain how the aircraft models are defined to control the joint structure properly.

3.1 Control law

Both aircraft will be flying in three different flight phases: joint hover, joint forward flight, and separate hover. A control law for both hover phases will need to be designed first, since joint forward flight can only be achieved after the joint hover phase is properly controlled.

For the flight control strategy, INDI is chosen as a starting point. INDI has proven to perform very well for tailsitter hybrid aircraft. These aircraft have complex aerodynamics during the different flight phases and are very sensitive to wind gusts in hover. INDI treats modeling errors as disturbances, to which it has good rejection capabilities [10, 13]. The following gives a brief overview of the control method, but the interested reader is referred to [13]. For both aircraft the following angular momentum equation holds:

$$
\begin{aligned}
M &= I_v \dot{\Omega} + \Omega \times I_v \Omega \\
&= M_a(\Omega, v) + M_c(\omega) + M_r(\omega, \dot{\omega}, \Omega),
\end{aligned} \tag{1}
$$

where M is the total moment, I_v is the inertia around the rotational axis of the aircraft, ω is the angular rate of the propellers around the body Z-axis and $\dot{\omega}$ is the angular acceleration of the propellers around the body Z-axis. M_a is the moment due to aerodynamics, M_c is the moment due to the controls, M_r is the moment due to the gyroscopic effect of the rotors and Ω is the angular rotation vector.

Eq. 1 can be used to derive the general control law of INDI, described as:

$$
\omega_c = \omega_f + (G_1 + G_2)^+ (v - \dot{\Omega}_f + G_2 z^{-1}(\omega_c - \omega_f)), \tag{2}
$$

where ω_c is the new motor command, ω_f is the filtered motor command of the previous iteration, G_1 describes the control effectiveness of the actuators, G_2 describes the propeller inertia effect on the Z-axis, $\dot{\Omega}_f$ is the filtered measured angular acceleration, and v is the virtual control input. This virtual control is defined as the reference angular acceleration created by a PD controller. A full derivation is given in [14].

3.2 Control authority analysis

To analyse how the two aircraft compare considering control authority, the control moment from Eq. 1 is used. Per axis, the control moment, M_c, is defined for a quadrotor as [15]:

$$
M_c = \begin{bmatrix} -bk_1 & bk_1 & bk_1 & -bk_1 \\ lk_1 & lk_1 & -lk_1 & -lk_1 \\ k_2 & -k_2 & k_2 & -k_2 \end{bmatrix} \omega^2, \tag{3}
$$

where b is the lateral distance from the Center of Gravity (CG) to the rotors, l is the longitudinal distance between the CG and the rotors, k_1 is the force constant of the rotors, k_2 is the moment constant of the rotors, and ω is the angular rate vector of the rotors.

From Eq. 3 the control effectiveness of the different actuators can be derived. The actuator force constants are the same for the biplane and the quadrotor, since the same hardware is used for both aircraft. If the control surfaces were negated, both the biplane and the quadrotor separately can be seen as two quadrotors, where Eq. 3 holds. Table 2 shows an overview of b and l for the biplane and the quadrotor.

	b	l
Biplane	0.74 [m]	0.11 [m]
Quadrotor	0.32 [m]	0.11 [m]

Table 2: lateral and longitudinal distances from rotor actuators to CG for the biplane and the quadrotor.

By comparing b and l in Table 2, it can be observed that it is only around the roll axis the biplane has more control authority than the quadrotor from the propellers alone. Furthermore, for pitch and yaw, the control surfaces of the biplane aid in control. In conclusion, in all rotational directions the biplane has more control authority than the quadrotor.

4 CONTROL STRATEGIES FOR THE QUADROTOR IN JOINT HOVER

One of the main difficulties of the project is the lack of intercommunication. It is deemed infeasible to let both UAVs track a reference model due to the difficulty of synchronisation and (different) sensor errors. As the UAV with the most control authority, the biplane is provided with a reference model to track.

The goal is to have the quadrotor improve the overall performance of the joint structure. Firstly, tracking performance and disturbance rejection behaviour is preferred for tailsitter platforms like the biplane. Secondly, the least amount of energy should be required to perform flight. Thirdly, the input commands should be as small as possible. Less required input command means that the actuators are further away from their saturation point, giving the actuators more room for extra manoeuvring.

The simplest strategy for the quadrotor is to provide a constant thrust, without creating any control moments. This makes the biplane fully responsible for the attitude control and adjusting the total amount of thrust. This control strategy will be referred to as *constant thrust*.

Due to the lack of communication, a major challenge for the quadrotor is to distinguish the difference between intended change in attitude or an external disturbance changing the attitude. Intended behaviour is created by changing reference signals, stemming from an outer-loop position controller or manual input from an RC controller. Unintended

behaviour is usually the result of external forces acting on the platform, for instance due to wind gusts. We will investigate if the quadrotor can improve the overall performance by resisting rotations, even though that means resisting intended rotations as well.

The next two investigated strategies are the *angular rate damper* and *angular acceleration damper*. These strategies will resist angular rates and angular accelerations respectively. The type of control is proportional control, as adding an integrator could lead to a steady state of opposing moments of the quadrotor and biplane.

Figure 4 shows the block diagrams for the three strategies. With the damper strategies, both the biplane and the quadrotor will detect a disturbance and will try to steer against this, though the quadrotor will also detect the intended behaviour of the biplane as a disturbance.

4.1 Control group for base reference

In order to compare the effect of the different quadrotor control strategies, performance has to be tested against a base reference. This base reference is one INDI attitude controller directly controlling *all eight rotor actuators and the control surfaces*. This makes the control group physically different from the three investigated control strategies for the quadrotor. For this strategy to work, the motors of the quadrotor are directly wired to the biplane. In the next sections this base reference is referred to as the *control group*.

4.2 Stability analysis

Figure 5 shows a Nichols plot derived for the different control strategies. This plot is created for the entire joint structure controller, as displayed in Figure 4. The goal is to have the system's frequency response be as far from the critical point, the red cross, in the middle. The vertical distance from the system's frequency response to the critical point illustrates the gain margin, and the horizontal distance defines the phase margin. It becomes clear that the angular acceleration damper strategy is the least robust, closely followed by the constant thrust strategy. The control group overlaps again with the constant thrust strategy. The angular rate damper is the most robust, showing better gain and phase margins than the control group.

5 PRACTICAL VERIFICATION

This section is focused on the joint structure's release mechanism and the test sequence for the control strategies. The test sequence has been simulated in Matlab prior to the practical flights, but will not be further mentioned due to the page restrictions for this paper.

5.1 Release Mechanism

The joint structure was built as per description mentioned in Section 2. The sequence of release is shown in Figure 6. It is important to note that the quadrotor does not control its attitude during the release. This is because the motor mount of the quadrotor has to slide off a carbon plate, as shown

in Figure 3, and if a moment is applied this causes friction. If the quadrotor was using attitude control, or even one of the damper strategies, it could steer against the biplane and through the generated moment obstruct proper detachment.

On average, the quadrotor was clear of the biplane within $0.39\,[sec]$. The total delay time before activation of the attitude controller was iteratively set to $0.5[sec]$. This left enough time for the quadrotor to be clear of the biplane and not be in free flight for too long without active attitude control. The set-up was tested with varying forward pitch angles up to $\theta = -18\,[deg]$. At 70% thrust, the quadrotor consistently released well.

The release system was also tested outdoors. The biplane was controlled by a separate pilot using an RC controller. At the moment of release, the goal was to have all the angles be as close to as possible to $[\phi, \theta, \psi] = [0, 0, 0]$ degrees. Figure 7 shows the three phases of the in-flight release. Next, both platforms were proven to be capable of separate flight. In the case of the biplane, hover flight was carried out with the four outer rotors and the control surfaces.

The biplane was tuned for flight with the quadrotor attached. This means that, for the calculated control effectiveness, the inertia of the joint structure is taken into account, including the mass of the quadrotor. When the quadrotor releases, the actual control effectiveness increases due to the decreased inertia. This effectively leads to a gain higher than 1 in the control system. According to Figure 5, there is some degree of robustness to such a gain change. In practice the flight performance of the biplane without the quadrotor proved adequate. One reason could be that the weight of the quadrotor sits close to the CG, which only leads to a small change in inertia once the quadrotor detaches.

5.2 Control strategies - test setup

Two experiments were performed: one to test the tracking performance and one to test disturbance rejection. For the first experiment, the intentional step input was initialised via the RC controller. The step was set to $\phi = 18\,[deg]$ in both positive and negative roll angles.

The experiments were performed indoors to avoid any influence of wind, in one sitting. In all cases, the thrust level for the quadrotor was set to 70%. Table 3 shows the mean throttle levels for the biplane for the various configurations.

Mean Throttle level	Biplane	Quadrotor
control group	62.13 [%]	-
ang. rate damper	53.90 [%]	70 [%]
constant thrust	53.90 [%]	70 [%]
ang. acc. damper	54.21 [%]	70 [%]
separate flight	72.33 [%]	40 [%]

Table 3: throttle levels for different configurations

In order to create a repeatable and consistent step disturbance a weight was dropped from the joint structure. Two identical weights of $672\,[g]$ each were put on the sides of the
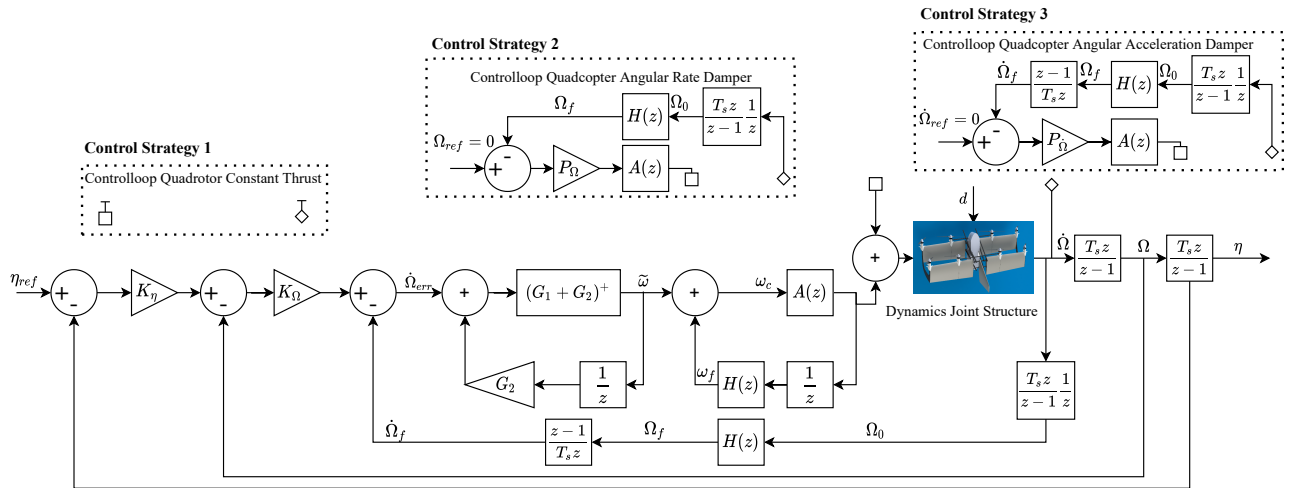
Figure 4: Three control strategies for the quadrotor. The lower section of the loop shows the INDI cascaded attitude controller of the biplane. The area within the dotted line resembles the control loop for the quadrotor.
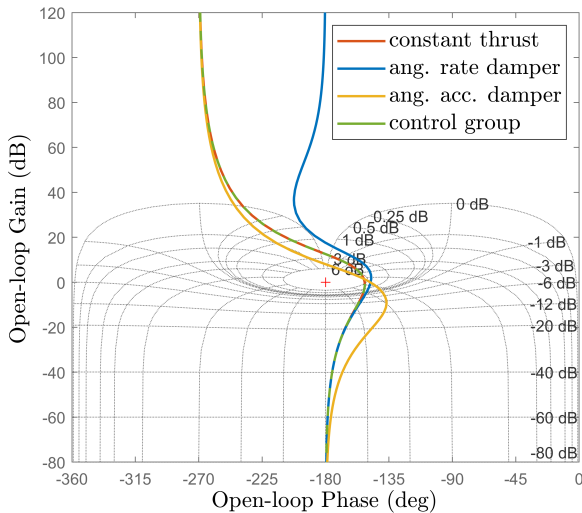

Figure 5: Nichols plot for three strategies. Constant thrust and the control group overlap. The angular rate damper strategy should provide the best stability.

biplane, one weight on each side. This created a net zero moment on the roll axis, not changing the CG, in the beginning of the test. After the release of one weight, the CG was shifted towards the weight that was still attached, resulting in a constant roll moment. This step disturbance is comparable to [16], but Smeur et al. added a weight to the aircraft.

An effort was made to keep the flight controller software similar for the different controllers to the greatest possible extent. The actuator dynamics, the filtering, and the sensor fusion all took place in a similar fashion for the quadrotor as well as the biplane. The main differences were the measurements and the actual control law.

5.3   Control strategies - test results

Figure 8 illustrates the overall result of all the roll angle step input tests. Figure 8a and 8b show the mean response and input command respectively of 6 repetitions for the angular rate and angular acceleration damper strategies, 5 repetitions for the control group and 3 repetitions for the constant thrust strategy. Table 4 and 5 show relevant parameters of the step input and disturbance.

Figure 8a shows that the step input tests give a very similar response for all the strategies. Overshoot for all of the strategies does not go above 5% of the step angle. The new steady-state roll angle could not be maintained for a long time, due to a lack of space in the hangar. This also explains why the initial roll angle does not show a good steady-state value for some responses.

The increase of the roll command after $t = 2\ [sec]$ can be explained by the fact that the joint structure needs to put in a constant roll offset to keep the roll angle at $\phi = 18\ [deg]$. This is referred to as a head-up moment, due to the flapping movement of the rotor [17].

Where the difference between strategies for the step responses is small, the difference for disturbance rejection is more significant. Table 5 shows that the control group has the lowest ϕ_{err}^{max} and the smallest required input command, as expected. Comparing this base reference strategy to the other strategies, we find that the constant thrust would require 19% more peak input command to counteract the disturbance. The angular acceleration damper strategy performs even worse at 27% more required peak input command. The angular rate
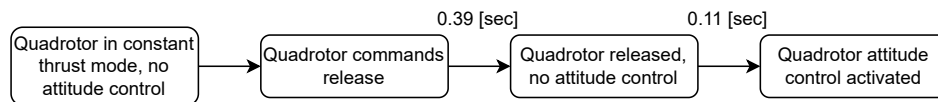
Figure 6: Flowchart of the release mechanism

(a) Joint hover; Biplane in attitude INDI and quadrotor constant 70% thrust.

(b) Release mechanism engaged; The quadrotor has no attitude control.

(c) Separate flight; Both aircraft are in attitude control.

Figure 7: Field release test

damper strategy performed the best, as it only required 11% more peak input command compared to the control group. The same order of performance can be stated for ϕ_{err}^{max} and the total energy required.

At this point it should be borne in mind that the control group for this study acted as a base reference only, not as a feasible option. Of the options that were deemed feasible, the angular rate damper strategy proved to be the best.

6   Conclusion

This paper proposes a combined aerial system consisting of a biplane and quadrotor attached together, that can hover cooperatively, and disassemble in-flight followed by separate flight. In-flight release worked consistently and is tested up to a forward pitch angle of -18 [deg]. Given the fact that no intercommunication is available, the angular rate damper control strategy for the quadrotor helps with disturbance rejection, while marginally affecting performance in terms of intended behaviour. Compared to the control group strategy, no active attitude control would result in 19% extra command. With the rate damper strategy active, this is reduced to 11% extra input command needed. Also, the maximum angle that the joint platform would reach due to the disturbance and the total amount of energy required is reduced with the active damper strategy. The angular acceleration damper strategy performed significantly worse for both the extra input command and the maximum angle.

7   Discussion, further research

The system is designed to also be able to fly in fast forward flight, but this has not been tested within the scope of this paper. Future work could investigate the stability and tracking performance during transition and forward flight as well. Additionally, future work could include examining how the quadrotor could be given more knowledge of the reference trajectory. This could be done with geofencing to let the quadrotor know what phase of flight the joint structure is in. One could raise the question if it is worth it to avoid communication between the drones, as the results show that it does come at the cost of a small degradation in performance. Additionally, without communication the biplane may reach saturation limits quicker, as it has lower control authority compared to the case where it can send a command to the quadrotor. Communication would also allow for the quadrotor to adjust the thrust setting to the most efficient level, instead of the constant value that it had in this paper.

References

[1] Mark Voskuijl, Muhammad R Said, Jaspreet Pandher, Michel J van Tooren, and Blin Richards. In-flight deployment of morphing uavs–a method to analyze dynamic stability, controllability and loads. In *AIAA Aviation 2019 Forum*, page 3126, 2019.

[2] Daniel Briggs Wilson, Ali Göktogan, and Salah Sukkarieh. Guidance and navigation for uav airborne docking. In *Robotics: Science and Systems*, volume 3, 2015.

[3] Ruibin Xue and Gaohua Cai. Formation flight control of multi-uav system with communication con-

	Settling time	Max. input command	Energy required for t=[1-3.5]
control group	0.89 [sec]	23.62 [%]	8.00 [%· s]
ang. rate damper	0.84 [sec]	22.76 [%]	8.18 [%· s]
constant thrust	0.84 [sec]	23.56 [%]	8.96 [%· s]
ang. acc. damper	0.81 [sec]	23.73 [%]	10.31 [%· s]

Table 4: Practical results for the different strategies for intended step inputs.

	Max. ϕ_{error}	Max. input command	Relative change	Energy required for t=[0-2.25]
control group	5.19 [deg]	26.64 [%]	100 [%]	31.44 [%· s]
ang. rate damper	5.79 [deg]	29.62 [%]	111 [%]	38.78 [%· s]
constant thrust	6.29 [deg]	31.67 [%]	119 [%]	40.38 [%· s]
ang. acc. damper	6.92 [deg]	33.84 [%]	127 [%]	42.62 [%· s]

Table 5: Practical results for the different strategies for disturbance rejection. For the input command, the relative change is given with respect to the base reference of the control group.

straints. *Journal of aerospace technology and management*, 8(2):203–210, 2016.

[4] Mohammad A Dehghani and Mohammad B Menhaj. Communication free leader-follower formation control of unmanned aircraft systems. *Robotics and Autonomous Systems*, 80:69–75, 2016.

[5] David Saldana, Bruno Gabrich, Guanrui Li, Mark Yim, and Vijay Kumar. Modquad: The flying modular structure that self-assembles in midair. In *2018 IEEE International Conference on Robotics and Automation (ICRA)*, pages 691–698. IEEE, 2018.

[6] Raymond Oung and Raffaello D'Andrea. The distributed flight array: Design, implementation, and analysis of a modular vertical take-off and landing vehicle. *The International Journal of Robotics Research*, 33(3):375–400, 2014.

[7] David Saldana, Parakh M Gupta, and Vijay Kumar. Design and control of aerial modules for inflight self-disassembly. *IEEE Robotics and Automation Letters*, 4(4):3410–3417, 2019.

[8] Atheer L. Salih, M. Moghavvemi, Haider A. F. Mohamed, and Khalaf Sallom Gaeid. Modelling and pid controller design for a quadrotor unmanned air vehicle. In *2010 IEEE International Conference on Automation, Quality and Testing, Robotics (AQTR)*, volume 1, pages 1–5, 2010.

[9] Hongwei Mo and Ghulam Farid. Nonlinear and adaptive intelligent control techniques for quadrotor uav–a survey. *Asian Journal of Control*, 21(2):989–1008, 2019.

[10] Christophe De Wagter, Bart Remes, Ewoud Smeur, Freek van Tienen, Rick Ruijsink, Kevin van Hecke, and Erik van der Horst. The nederdrone: A hybrid lift, hybrid energy hydrogen uav. *international journal of hydrogen energy*, 46(29):16003–16018, 2021.

[11] Hang Zhang, Bifeng Song, Haifeng Wang, and Jianlin Xuan. A method for evaluating the wind disturbance rejection capability of a hybrid uav in the quadrotor mode. *International Journal of Micro Air Vehicles*, 11:1756829319869647, 2019.

[12] Bart Theys, Cyriel Notteboom, Menno Hochstenbach, and Joris De Schutter. Design and control of an unmanned aerial vehicle for autonomous parcel delivery with transition from vertical take-off to forward flight. *International Journal of Micro Air Vehicles*, 7(4):395–405, 2015.

[13] Ewoud JJ Smeur, Guido CHE de Croon, and Qiping Chu. Cascaded incremental nonlinear dynamic inversion for mav disturbance rejection. *Control Engineering Practice*, 73:79–90, 2018.

[14] Ewoud JJ Smeur, Qiping Chu, and Guido CHE de Croon. Adaptive incremental nonlinear dynamic inversion for attitude control of micro air vehicles. *Journal of Guidance, Control, and Dynamics*, 39(3):450–461, 2016.

[15] Robert Mahony, Vijay Kumar, and Peter Corke. Multirotor aerial vehicles: Modeling, estimation, and control of quadrotor. *IEEE Robotics and Automation magazine*, 19(3):20–32, 2012.

[16] EJJ Smeur. *Incremental Control of Hybrid Micro Air Vehicles*. PhD thesis, Delft University of Technology, 2018.

[17] Hikaru Otsuka, Daisuke Sasaki, and Keiji Nagatani. Reduction of the head-up pitching moment of small quadrotor unmanned aerial vehicles in uniform flow. *International Journal of Micro Air Vehicles*, 10(1):85–105, 2018.
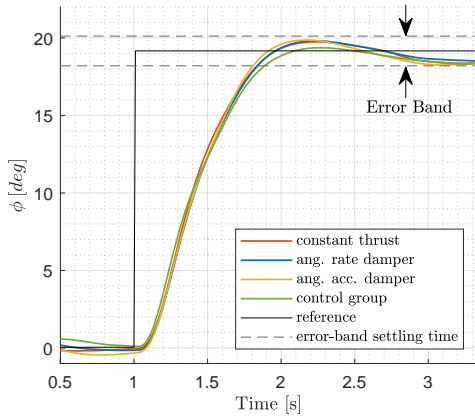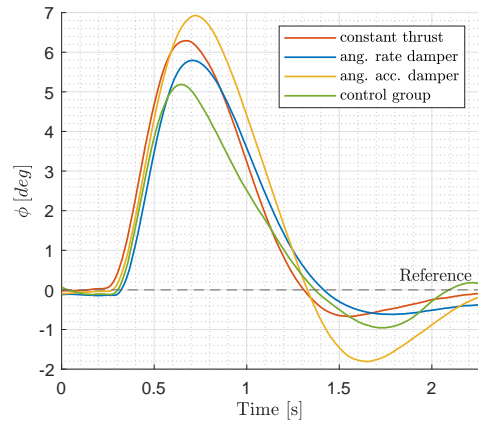
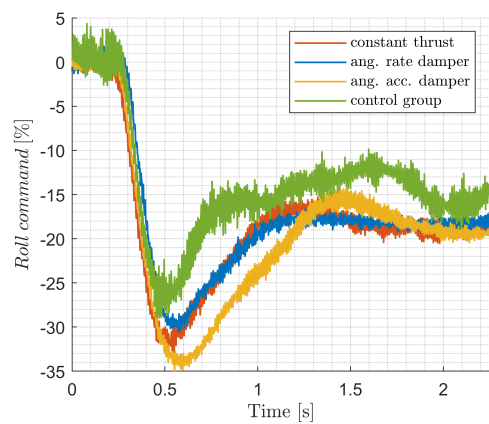(a) Roll angle after intended step input with a 5 % error band.
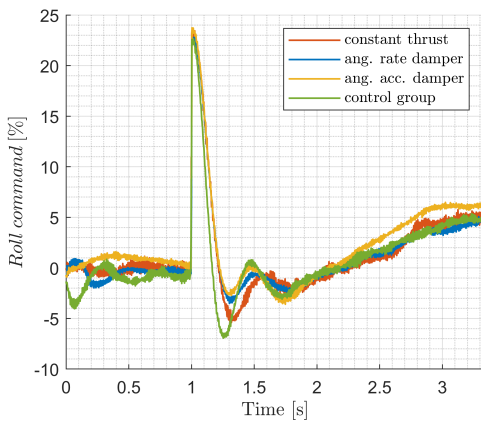
(b) Roll input command during intended step input. After 2 [sec] the input gradually increases due as the UAV picks up speed.

Figure 8: Intended step input in the Hover phase.

(a) Roll angle for disturbance rejection.

(b) Roll input command for disturbance rejection.

Figure 9: Intended step disturbance rejection in the Hover phase.